

# Revealing microscopic origins of shape coexistence in the Ni isotopic chain

Silvia Leoni<sup>1,\*</sup>, Bogdan Fornal<sup>2</sup>, Nicolae Marginean<sup>3</sup>, Michele Sferrazza<sup>4</sup>, Yusuke Tsunoda<sup>5</sup> and Takaharu Otsuka<sup>5,6,7,8,9</sup>

<sup>1</sup> Department of Physics, University of Milano and INFN, Via Celoria 16, 20133, Milano, Italy

<sup>2</sup> Institute of Nuclear Physics, PAN, 31-342 Kraków, Poland

<sup>3</sup> Horia Hulubei National Institute of Physics and Nuclear Engineering - IFIN HH, Bucharest 077125, Romania

<sup>4</sup> Département de Physique, Université libre de Bruxelles, B-1050 Bruxelles, Belgium

<sup>5</sup> Center for Nuclear Study, University of Tokyo, Hongo, Bunkyo-ku, Tokyo 113-0033, Japan

<sup>6</sup> Department of Physics, University of Tokyo, Hongo, Bunkyo-ku, Tokyo 113-0033, Japan

<sup>7</sup> RIKEN Nishina Center, 2-1 Hirosawa, Wako, Saitama 351-0198, Japan

<sup>8</sup> Instituut voor Kern- en Stralingsfysica, KU Leuven, B-3001 Leuven, Belgium

<sup>9</sup> National Superconducting Cyclotron Laboratory, Michigan State University, East Lansing, Michigan 48824, USA

**Abstract.** In a two-neutron transfer experiment, performed in Bucharest in July 2016 at sub-Coulomb barrier energy, a photon decay hindered - solely - by a nuclear shape change was identified in the <sup>66</sup>Ni nucleus. Such a rare process, at spin zero, was clearly observed before only in actinide nuclei in the 1970's, where fission isomers were found. The experimental findings on <sup>66</sup>Ni have been well reproduced by the Monte Carlo Shell Model Calculations of the Tokyo group, which predict a multifaceted scenario of coexistence of spherical, oblate and prolate shapes in neutron-rich Ni isotopes. The results on <sup>66</sup>Ni encouraged a comprehensive gamma-spectroscopy investigation of neutron-rich Ni isotopes, in particular <sup>62</sup>Ni and <sup>64</sup>Ni, at IFIN-HH (Bucharest), IPN Orsay and ILL (Grenoble), employing different reaction mechanisms to pin down the wave function composition of selected excited states. The aim is to shed light on the microscopic origin of deformation in neutron-rich Ni nuclei, possibly locating other examples of “shape-isomer-like” structures in this region.

## 1 Introduction

The shape is one of the most fundamental properties of the atomic nucleus. Spherical shapes naturally appear in the vicinities of magic nuclei. On the contrary, when moving away from shell closures, different shapes may compete, and often coexist in the very same nucleus at low spins, in a restricted interval of low excitation energy [1,2]. Shapes of quadrupole symmetric forms are the most abundant, a special class being represented by superdeformed states: they have been experimentally observed next to spherical/oblate excitations at high spin and high energy, even in the proximity of magic numbers [3-5].

Low-lying 0<sup>+</sup> excited states, characterized by deformations different from the ground state, represent one of the most striking fingerprints of shape coexistence, in even-even systems. They have been discovered in different regions of the nuclear chart, from the “light” Si/Mg and Ni/Zn/Ge regions, to the much heavier Po/Pb/Hg and Rn/Ra systems. Indeed, it is in the U region that, back in the 60's, the first and most striking examples of shape coexistence, namely shape isomers, were discovered. In <sup>236</sup>U and <sup>238</sup>U, E2  $\gamma$  branches from excited 0<sup>+</sup> states showed a retardation of the order of 10<sup>7</sup>, in competition with fission [6-8]. Such states were interpreted as deformed structures, residing in secondary minima of the nuclear potential energy surface (PES), separated by a high barrier from the main ground state configuration [9]. Shape isomerism has been predicted to occur also in other regions of the nuclear chart, in particular in the neutron-rich Ni region, by various mean-field models [10-12]. However, it is only very recently that an example of “shape-isomer-like” structure was found by our collaboration in the <sup>66</sup>Ni nucleus [13],

while coexistence of spherical, oblate and prolate shapes along the Ni isotopic chain was observed in experiments performed at ISOLDE/CERN, MSU and RIKEN [14-16]. The phenomenon of shape coexistence in neutron-rich Ni isotopes can nowadays be also described by fully microscopic approaches, taking advantage of the most powerful supercomputing systems. One of the most prominent examples is the Monte Carlo Shell Model (MCSM) of the Tokyo group [17], which correctly predicts the occurrence of shape isomerism in <sup>66</sup>Ni, together with other possible cases in the lighter <sup>62,64</sup>Ni stable isotopes, although with reduced magnitude.

In this proceeding we report on the research program of our collaboration, aiming at a detailed investigation, with different probes, of the microscopic structure of neutron-rich Ni isotopes, from mass A=62 to A=66. After recalling the observation of a “shape-isomer-like” structure in <sup>66</sup>Ni [13], obtained in a 2016 experiment performed at the Tandem Laboratory of the Horia Hulubei National Institute of Physics and Nuclear Engineering (IFIN-HH), in Bucharest, we briefly describe the following series of measurements on the Ni chain, currently ongoing in Bucharest, IPN-Orsay and ILL (Grenoble). The aim of this research program is to shed light on the microscopic origin of nuclear deformation, not least shape isomerism, using different reaction mechanisms, to probe MCSM predictions.

\* Corresponding author: [silvia.leoni@mi.infn.it](mailto:silvia.leoni@mi.infn.it)

## 2 Experimental Investigation

The research program of our collaboration concerns the detailed spectroscopic investigation of neutron-rich Ni nuclei, from  $^{62}\text{Ni}$  to  $^{66}\text{Ni}$ , by employing sub-Coulomb barrier transfer reactions with heavy-ion stable beams and neutron capture reactions with intense neutron beams (see Fig. 1). Particular emphasis is given to lifetime measurements, as well as to comparative studies of the population of specific states by different reaction mechanisms (e.g., proton and neutron transfer reactions with  $^{11}\text{B}$  and  $^{18}\text{O}$  heavy ions). Such reactions are found to selectively populate specific excited states, thus suggesting a sensitivity to the state wave function composition.

We like to note that similar spectroscopy measurements in heavier Ni isotopes (see Fig. 1) would necessarily require intense radioactive beams from new generation facilities, such as SPES, HIE-ISOLDE or SPIRAL2.

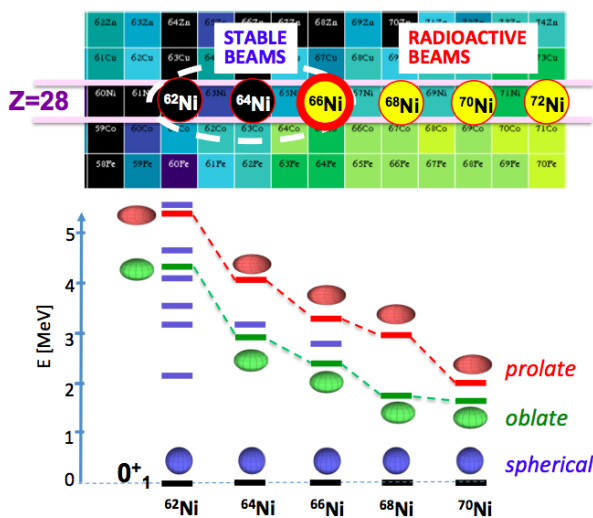


**Fig. 1.** Top: region of the nuclear chart focusing on neutron-rich Ni isotopes in the proximity of the valley of stability. Even-even  $A=62, 64, 66$  (and the even-odd 65), are currently investigated by the present collaboration, employing intense stable ion beams and neutron beams. Heavier Ni isotopes require, instead, intense radioactive beams. Bottom: Monte Carlo Shell Model predictions for  $0^+$  states of spherical (blue), oblate (green) and prolate (red) shape, for Ni isotopes between  $A = 62$  and 70.

### 2.1. Spectroscopy of $^{62}\text{Ni}$ , $^{64}\text{Ni}$ and $^{66}\text{Ni}$ by two-neutron transfer reactions

The first experiment of this research program, on the Ni chain, was performed by our collaboration in July 2016, at the Tandem Laboratory of IFIN-HH, in Bucharest. It focused on the spectroscopy of  $^{66}\text{Ni}$  populated by the two-neutron transfer reaction induced by a  $^{18}\text{O}$  beam on a  $^{64}\text{Ni}$  target, at the sub-Coulomb barrier energy of 39 MeV [13]. This low energy severely hindered the fusion-evaporation channel. The experiment made use of a steady beam current of about 30 pA, for more than 40 days and the  $\gamma$ -decay from excited states in  $^{66}\text{Ni}$  was measured with the ROSPHERE HPGe array [18], consisting at that time of 14 HPGe detectors and 11 LaBr<sub>3</sub>(Ce) scintillators. The first part of the experiment was performed with a 5 mg/cm<sup>2</sup> thick target, in order to

obtain a very clean spectrum by gating on the 1425-keV  $2^+ \rightarrow 0^+$  ground state transition. All observed transitions were found to belong to  $^{66}\text{Ni}$  and depopulate states reported by Broda et al. [19] at excitation energy below  $\approx 4.1$  MeV. After a closer inspection of the gamma-ray spectra, several transitions clearly showed tails, pointing to emission in flight during the slowing down process of  $^{66}\text{Ni}$  inside the target. By using a Doppler Shift Attenuation Method (DSAM) lineshape analysis [20-21], half lives values in the range from 1 to 2 ps were obtained for a total of six states, i.e., the 7-, 3+, 4+, 2+, 4+ and 3-states at 4089, 2971, 3185, 3229, 3614 and 3687 keV depopulated by the 490-, 1546-, 1760-, 1804-, 2189- and 2262-keV lines, respectively. Extracted  $B(E/M\lambda)$  values resulted in fair agreement with MCSM predictions, as shown in Table 1 (for the 3- state at 3687 keV, no predictions are available). This analysis gives strong support to the predictive power of the model, which turns out to reproduce extremely well also the beta-decay properties of  $^{66}\text{Co}$  into  $^{66}\text{Ni}$  [22].

In the second part of the experiment, the lifetimes of all three  $0^+$  excited states (located at 2443-, 2671- and 2974-keV excitation energies, respectively) were extracted via the plunger technique, using the same  $^{18}\text{O}+^{64}\text{Ni}$  reaction and a 5 mg/cm<sup>2</sup> thick Ta stopper, placed between 10 and 3000  $\mu\text{m}$  from a 1 mg/cm<sup>2</sup>  $^{64}\text{Ni}$  target (12 distances were considered). Half lives values of 7.6(8), 134(9) and 20(7) ps were obtained, corresponding to  $B(E2)$  decay probabilities of  $4.3\pm 0.5$ ,  $0.09\pm 0.01$ , and  $0.21\pm 0.07$  W.u., for the  $0_2^+$ ,  $0_3^+$  and  $0_4^+$  states, respectively. In the case of  $0_3^+$ , the independent measurement of Olaizola et al. [23] confirmed our value. Table 1 summarizes the results obtained from the lifetime analysis of  $^{66}\text{Ni}$ .

A detailed analysis of the wave functions composition of the excited  $0^+$  states, calculated by the MCSM, was then performed to interpret the experimental results. It turned out that in the case of  $0_3^+$ , the retardation of the E2 decay is arising from cancellation effects among E2 matrix elements, while for the  $0_4^+$  state located at 2974 keV, the hindrance is of different nature. In this case, it is caused by a sizable barrier in the potential energy surface (PES), separating a deep prolate secondary minimum, in which the  $0_4^+$  resides, from the spherical ground state minimum. Further, it was found that this prolate local minimum of  $0_4^+$  arises from a promotion of neutrons up to the  $g_{9/2}$  orbital, what reduces the proton shell gap at  $Z=28$  and, in consequence, favors the promotion of protons across this gap [17]. Such a result makes  $^{66}\text{Ni}$  a unique example of nuclear system, apart from the much heavier actinides, in which a photon decay is hindered - solely - by a nuclear shape change (a “shape-isomer-like” structure). Figure 2, on the right, shows a comparison between a partial level scheme of  $^{66}\text{Ni}$ , focusing on the decay from the  $0^+$  states, and predictions from the MCSM.

As shown in the bottom of Fig. 1, MCSM calculations predict a scenario of coexisting shapes also in  $^{62}\text{Ni}$  and  $^{64}\text{Ni}$ , with the possible appearance of “shape-isomer-like” structures similarly to the case of  $^{66}\text{Ni}$ , although occurring at higher excitation energy and with reduced magnitude. In  $^{64}\text{Ni}$ , as in  $^{66}\text{Ni}$ , the first three excited  $0^+$  states are calculated to be oblate, spherical and prolate, respectively, while in  $^{62}\text{Ni}$  up to 9 excited  $0^+$

	E [keV]	T <sub>1/2</sub> [ps]	E <sub>γ</sub> [keV]	I <sub>i</sub> → I <sub>f</sub> (E/Mλ)	B(E/Mλ) <sub>exp.</sub> [W.u.]	B(E/Mλ) <sub>Th.</sub> [W.u.]
PLUNGER	2443	7.6(8)	1018	0 <sup>+</sup> → 2 <sup>+</sup> (E2)	4.3(5)	4.1
PLUNGER	2671	134(9)	1245	0 <sup>+</sup> → 2 <sup>+</sup> (E2)	0.09(1)	0.01
PLUNGER	2974	20(7)	1549	0 <sup>+</sup> → 2 <sup>+</sup> (E2)	0.21(7)	0.006
PLUNGER	3541	1456(478)	356	5 <sup>-</sup> → 4 <sup>+</sup> (E1)	6.0 × 10 <sup>-6</sup>	-
DSAM	2971	0.9(1)	1546	3 <sup>+</sup> → 2 <sup>+</sup> (M1)	6.3(7) × 10 <sup>-3</sup>	2.8 × 10 <sup>-3</sup>
DSAM	3185	1.4(1)	1760	4 <sup>+</sup> → 2 <sup>+</sup> (E2)	1.5(1)	5.9
DSAM	3229	1.5(2)	1804	2 <sup>+</sup> → 2 <sup>+</sup> (M1)	2.5(4) × 10 <sup>-3</sup>	2.4 × 10 <sup>-3</sup>
DSAM	3614	0.6(1)	2189	4 <sup>+</sup> → 2 <sup>+</sup> (E2)	1.1(1)	0.74
DSAM	3687	0.9(1)	2262	3 <sup>-</sup> → 2 <sup>+</sup> (E1)	3.9(5) × 10 <sup>-5</sup>	-
DSAM	4089	1.3(2)	490	7 <sup>-</sup> → 6 <sup>-</sup> (M1)	0.15(2)	0.073

**Table 1.** Summary of the <sup>66</sup>Ni lifetime analysis results obtained with Plunger (top) and DSAM (bottom) techniques, in comparison with theory predictions from MCSM [17].

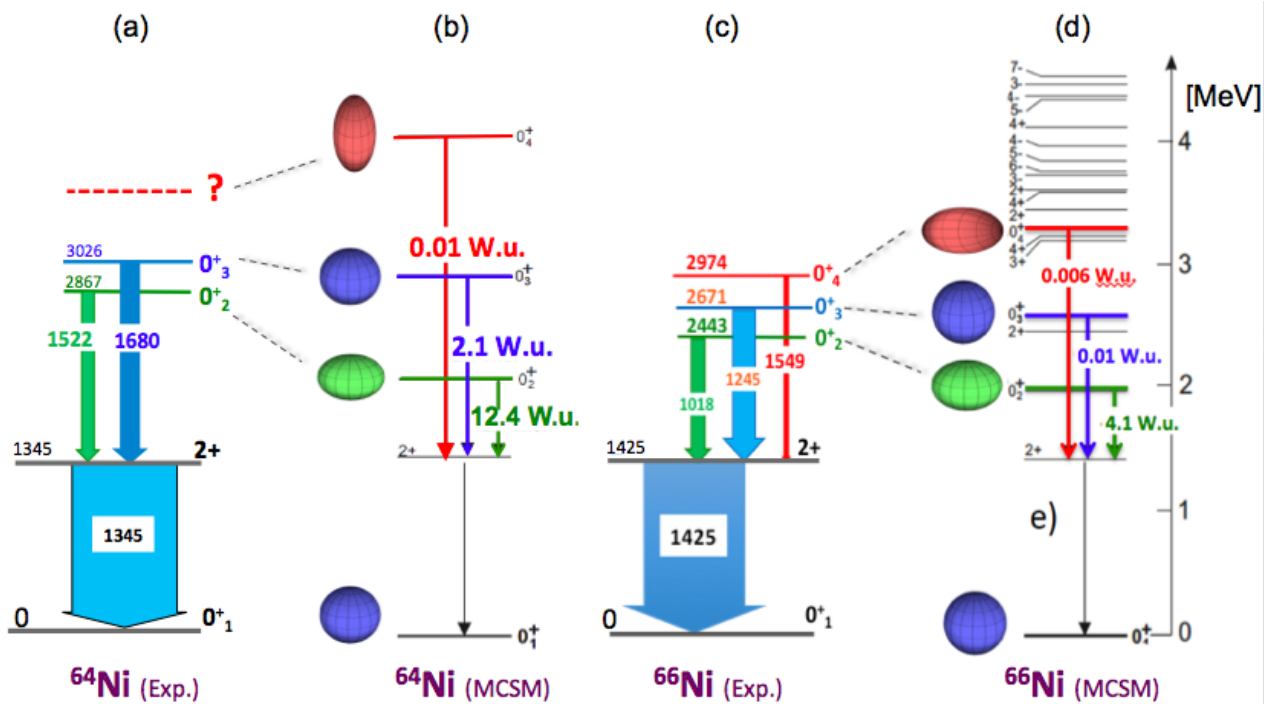


**Figure 2.** Partial level schemes of <sup>64</sup>Ni (a) and <sup>66</sup>Ni (c), focusing on the decay from 0<sup>+</sup> states, as observed experimentally. Corresponding calculations from Monte Carlo Shell Model are shown in (b) and (c), with cartoons indicating the predicted intrinsic shape for the 0<sup>+</sup> states (i.e., spherical (blue), oblate (green) and prolate (red)). Calculated B(E2) values from each 0<sup>+</sup> excitation to the first excited 2<sup>+</sup> state are also given in Weisskopf units (W.u.).

states are expected. They are all predicted to be spherical, apart from  $0_6^+$  and  $0_8^+$ , which should be characterized by oblate and prolate shapes, respectively. According to calculations,  $^{62}\text{Ni}$  should mark the appearance of coexisting deformations in the Ni isotopes, in the neutron rich side of the nuclear chart.

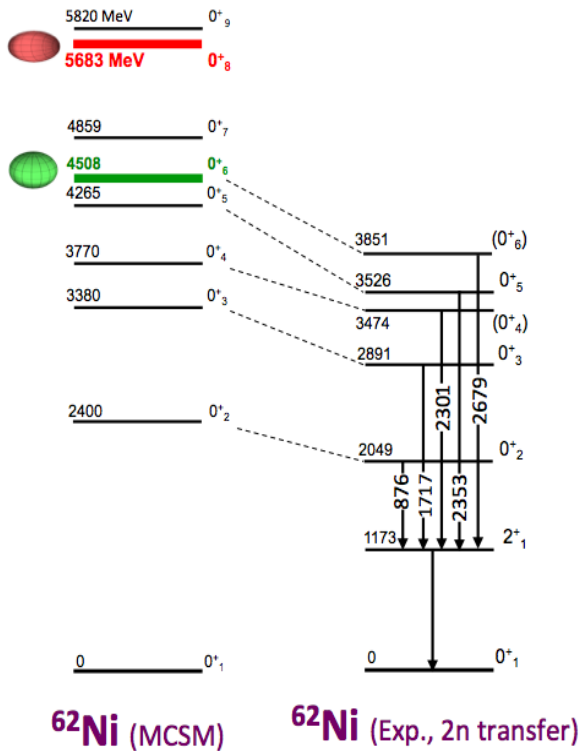


**Figure 3.** Preliminary comparison between MCSM predictions (left) and experimental data (right) for excited  $0^+$  states in  $^{62}\text{Ni}$ . The experiment was performed with the Nu-Ball array at ALTO IPN-Orsay, employing the 2n-transfer reaction  $^{60}\text{Ni}(^{18}\text{O},^{16}\text{O})^{62}\text{Ni}$ , at sub-Coulomb barrier energy.

Encouraged by the above predictions, our collaboration has started a detailed investigation of  $0^+$  excitations in  $^{62}\text{Ni}$  and  $^{64}\text{Ni}$ , by employing two-neutron transfer reactions, at sub-Coulomb barrier energy, with a  $^{18}\text{O}$  beam on  $^{60}\text{Ni}$  and  $^{62}\text{Ni}$  targets. The  $^{64}\text{Ni}$  experiment was performed at IFIN-HH, with the ROSPHERE array [18], while the  $^{62}\text{Ni}$  investigation was carried out at ALTO IPN-Orsay, with the Nu-Ball array, consisting of 24 Compton-suppressed HPGe Clover detectors (from EUROBALL), 10 Compton-suppressed HPGe coaxial detectors and 20  $\text{LaBr}_3$  scintillator detectors, for lifetime measurements by fast-timing techniques.

Figures 2 (left) and 3 show preliminary results from the analysis of  $^{64}\text{Ni}$  and  $^{62}\text{Ni}$  two neutron-transfer data, in comparison with MCSM predictions. In the case of  $^{64}\text{Ni}$ , the decay from the second and third excited  $0^+$  states, located at 2867 and 3026 keV, is clearly observed (see also top panel of Fig. 5), while no firm conclusions can be drawn, thus far, on the location of the prolate deformed  $0^+$  state, predicted by theory around 4 MeV. Preliminary results from plunger measurements provide lifetime values in the ps range for both  $0_2^+$  and  $0_3^+$ , in fair agreement with MCSM calculations, thus giving further support to their predictive power.

In the case of  $^{62}\text{Ni}$ , a preliminary spectroscopic investigation allowed to identify the  $\gamma$  decay from the first 5 excited  $0^+$  states, i.e.,  $0_2^+$  to  $0_6^+$  (see Fig. 3 and Fig. 4) - the spin assignment of the proposed  $0_4^+$  is being confirmed by angular correlation studies. According to MCSM calculations, the highest observed  $0^+$  excitation, i.e., the  $0_6^+$  state, should be of oblate nature, while the prolate  $0^+$  state, i.e.,  $0_8^+$  should be more than 1 MeV higher in excitation energy. It is interesting to note that one of the two  $0^+$  states, predicted to be deformed by the MCSM, could be the band head of the positive parity rotational band recently identified by Albers et al. in a high-spin experiment performed with GAMMASPHERE and FMA [24]. If this scenario is experimentally confirmed, the connection between deformation, developing at high spins, and the occurrence of coexisting shapes, at spin 0, could be established for the first time.

## 2.2. Selectivity of transfer reactions

In order to gain further insight into the structure of the excited  $0^+$  states, observed in  $^{62,64}\text{Ni}$  in the 2n transfer studies discussed above, proton-pick-up measurements induced by a  $^{11}\text{B}$  beam on  $^{63}\text{Cu}$  and  $^{65}\text{Cu}$  targets, at sub-Coulomb barrier energy, were performed in 2018 and 2019 at IFIN-HH. As shown in Figs. 4 and 5, a different selectivity in the population of excited states in  $^{62}\text{Ni}$  and  $^{64}\text{Ni}$  is clearly observed when comparing the spectra from the two-neutron transfer and one-proton pick-up reactions. As a general feature, in both nuclei the population of negative parity states is found to be strongly suppressed in the proton-pick-up reaction (see, for example, the 1825-keV  $5^- \rightarrow 4^+$  decay in  $^{62}\text{Ni}$ , in Fig. 4, and the 1475-keV  $5^- \rightarrow 4^+$  or the 2213-keV  $3^- \rightarrow 2^+$  decays in  $^{64}\text{Ni}$ , in Fig. 5).

What concerns the  $0^+$  states, in both  $^{62}\text{Ni}$  and  $^{64}\text{Ni}$  a clear change in their relative population is observed, when comparing the two-neutron-transfer and one-proton-pick-up reactions. For both nuclei, the proton-pick-up reaction strongly suppresses the population of certain  $0^+$  states, i.e.,  $0_3^+$  in  $^{62}\text{Ni}$ , and both  $0_2^+$  and  $0_3^+$  in  $^{64}\text{Ni}$  (only the 1521-keV  $\gamma$  ray from  $0_2^+$  is weakly seen), as shown in Figs. 4 and 5.

Finally, the most striking feature, when comparing the two different transfer reactions, is the appearance of new transitions in the proton-pick-up case. In  $^{64}\text{Ni}$ , for example, two  $\gamma$  transitions are observed at 2138 and 2502 keV, which are not seen in the two-neutron-transfer reaction (see Fig. 5). They would depopulate states at 3484 and 3848 keV, respectively. The 2502-keV line is particularly strong and shows pronounced tails, what points to a lifetime comparable to the stopping time of the  $^{64}\text{Ni}$  product in the target (i.e.,  $\leq 1$  ps).

We like to note that Monte Carlo Shell Model Calculations may provide a first interpretation of the selective population observed in the proton-pick-up reactions, both for  $^{62}\text{Ni}$  and  $^{64}\text{Ni}$ . According to MCSM predictions, the structure of  $^{63}\text{Cu}$  and  $^{65}\text{Cu}$  - our target nuclei - is different: while the wave function of the  $3/2^-$  ground state of  $^{63}\text{Cu}$  shows fragmented contributions distributed over spherical and (slightly deformed) oblate and prolate configurations, the ground state of  $^{65}\text{Cu}$  is expected to exhibit a more defined spherical-oblate structure. This may play a role in determining the relative population of the different observed states (including  $0^+$

states) in the final  $^{62}\text{Ni}$  and  $^{64}\text{Ni}$  nuclei, after a proton removal from the ground state of  $^{63}\text{Cu}$  and  $^{65}\text{Cu}$ , respectively. In particular, it is found that the observed relative population of specific states in  $^{62}\text{Ni}$  and in  $^{64}\text{Ni}$ , could be, at least partially, explained, by looking at the Spectroscopic Factors (SF) predicted by the MCSM – they define the overlap between the initial state (i.e., the ground state of the target nucleus) and the final state wave functions. For example, in  $^{62}\text{Ni}$ , the direct population of  $0^+_3$  and  $0^+_4$ , with respect to  $0^+_2$ , is about 0.2(1) and 1.1(1), to be compared with the corresponding 0.2 and 2.2 SF's ratios. Similarly, in  $^{64}\text{Ni}$ , the experimental population of  $0^+_3$  with respect to  $0^+_2$  is about 0.1(1), while the SF's ratio gives 0.03. Such qualitative observations support the need for a detailed comparison between experiment and theory, in which both the microscopic structure of the state of interest and the specific features of the reaction mechanism are carefully taken into account.

To shed more light on the complex structure of both  $^{62}\text{Ni}$  and  $^{64}\text{Ni}$ , further experimental investigations are planned, in order to fully characterize the newly located excitations – they include neutron capture reactions with intense neutron beams at Institut Laue-Langevin (ILL, Grenoble), where the FIPPS HPGc array [25] can be used for high-precision  $\gamma$ -spectroscopy measurements.

### 3 Conclusion

A photon decay from a  $0^+$  state in  $^{66}\text{Ni}$ , hindered, solely, by a nuclear shape change, has been recently discovered by our collaboration [17]. This is a clear-cut evidence of a “shape-isomer-like structure”, an extremely rare case of totally different microscopic configurations (prolate and spherical in this case) coexisting at similar excitation energy. This experimental finding is well described by large scale shell model calculations based on Monte Carlo computational schemes, which provide a microscopic description of neutron-rich Ni isotopes and predict a coexistence of spherical, oblate and prolate structures along the entire chain. According to calculations, a deep prolate (secondary) minimum could also appear in lighter even-even neutron-rich Ni isotopes, such as  $^{62}\text{Ni}$  and  $^{64}\text{Ni}$ , although at higher excitation energies and with possibly reduced magnitude.

Inspired by the above results, our collaboration has started an extended research program aiming at a high-precision  $\gamma$ -spectroscopy investigation of neutron rich Ni isotopes, from  $A = 62$  to 66. Experimental campaigns are currently ongoing in Bucharest, ALTO IPN-Orsay and ILL (Grenoble), employing different reaction mechanisms to probe the state wave function composition. Preliminary results clearly show a different/strong selectivity in the population of specific states, when using reactions involving transfer of neutrons or protons, thus pointing to the need of a theoretical interpretation in which both structural properties and reaction dynamics are properly taken into account.

It is quite certain that such a detailed experimental investigation, performed with a strong support from theory, will significantly contribute to our understanding of the microscopic origin of nuclear deformation, a key issue in nuclear structure physics.

This work was supported by the Italian Istituto Nazionale di Fisica Nucleare, by the Polish National Science Centre under Contracts No. 2014/14/M/ST2/00738 and No. 2013/08/M/ST2/00257, by the Romanian MCI Project Nucleu PN 19 06 01 02 and by the Interuniversity Attraction Poles Programme (IAP) via the Belgian Science Policy Office (BriX network P7/12). It was supported by the Grants No. PN-II-RU-TE-2014-4-2003 and No. PNIII-IFA-CERN-RO-03-ISOLDE. It was also partially supported by Grants-in-Aid for Scientific Research (23244049), by HPCI Strategic Program (hp150224), by MEXT and JICFuS, by Priority Issue (Elucidation of the fundamental laws and evolution of the universe) to be Tackled by Using Post “K” Computer (hp160211, hp170230), and by CNS-RIKEN joint project for largescale nuclear structure calculations.

### References

1. J.L. Wood et al., Phys. Rep. **215**, 101 (1992).
2. K. Heyde and J. L. Wood, Rev. Mod. Phys. **83**, 1467 (2011).
3. B. Singh, R. Zywina, and R.B. Firestone, Nuclear Data Sheets **97**, 241 (2002).
4. A. Lopez-Martens et al., Prog. Part. Nuc. Phys. **89**, 137 (2016).
5. S. Leoni and A.Lopez-Martens, Phys. Scr. **91**, 063009 (2016).
6. S. M. Polikanov, Sov. Phys. Usp. **15**, 486 (1973).
7. J. Kantele et al., Phys. Rev. Lett. **51**, 91 (1983).
8. P. Butler et al., J. Phys. G **6**, 1165 (1980).
9. P. Walker and J. Dracoulis, Nature **399**, 35 (1999).
10. P. Bonche et al., Nucl. Phys. A **500**, 308 (1989).
11. M. Girod et al., Phys. Rev. Lett. **62**, 2452 (1989).
12. P. Möller et. al., Phys. Rev. Lett. **103**, 212501 (2009).
13. S. Leoni, B. Fornal, N. Marginean et al., Phys. Rev. Lett. **118**, 162502 (2017).
14. B. P. Crider et al., Phys. Lett. B **763**, 108 (2016).
15. A.I. Morales et al., Phys. Rev. C **93**, 034328 (2016).
16. A.I. Morales et al., Phys. Lett. B **765**, 328 (2017).
17. Y. Tsunoda et al., Phys. Rev. C **89**, 031301 (2014).
18. D. Bucurescu et al., Nuc. Inst. Meth. Phys. Res. A **837**, 1 (2016).
19. R. Broda et al., Phys. Rev. C **86**, 064312 (2012).
20. P. Petkov et al., Nuc. Inst. Meth. Phys. Res. A **488**, 555 (2002).
21. P. Petkov et al., Nuc. Inst. Meth. Phys. Res. A **783**, 6 (2015).
22. M. Stryczyk et al., Phys. Rev. C **98**, 064326 (2018).
23. B. Olaizola et al., Phys. Rev. C **95**, 061303(R) (2017).
24. M. Albers et al., Phys. Rev. C **94**, 034301 (2016).
25. C. Michelagnoli et al., EPJ Web Conf. **193**, 04009 (2018).

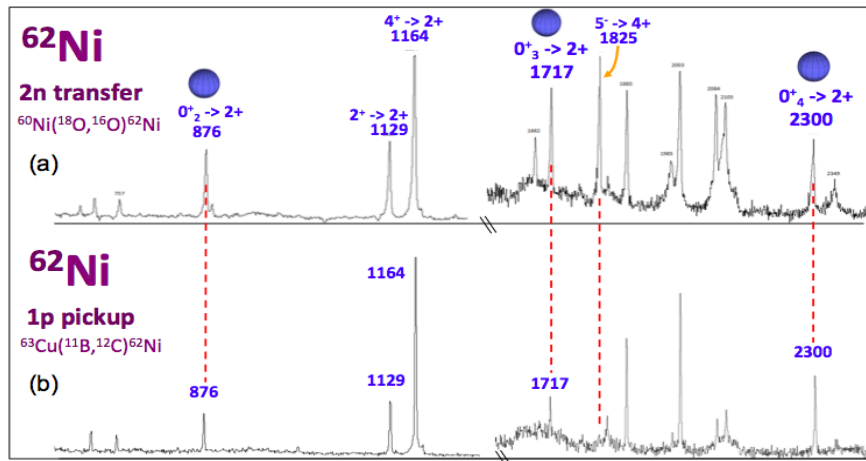


**Figure 4.** Portions of  $\gamma$  spectra of  $^{62}\text{Ni}$ , as obtained from the two-neutron transfer reaction  $^{60}\text{Ni}(^{18}\text{O},^{16}\text{O})^{62}\text{Ni}$  (a) and the proton pick-up reaction  $^{63}\text{Cu}(^{11}\text{B},^{12}\text{C})^{62}\text{Ni}$  (b) (both performed at beam energies  $\sim 1$  MeV below the Coulomb barrier energy), focusing on the transition energy region where the decay from the first three excited  $0^+$  states is expected. A clear difference in population pattern is generally observed, with strong suppression of transitions from negative parity states, in the case of the proton pick-up reaction (see for example the 1825-keV  $5^- \rightarrow 4^+$  decay).

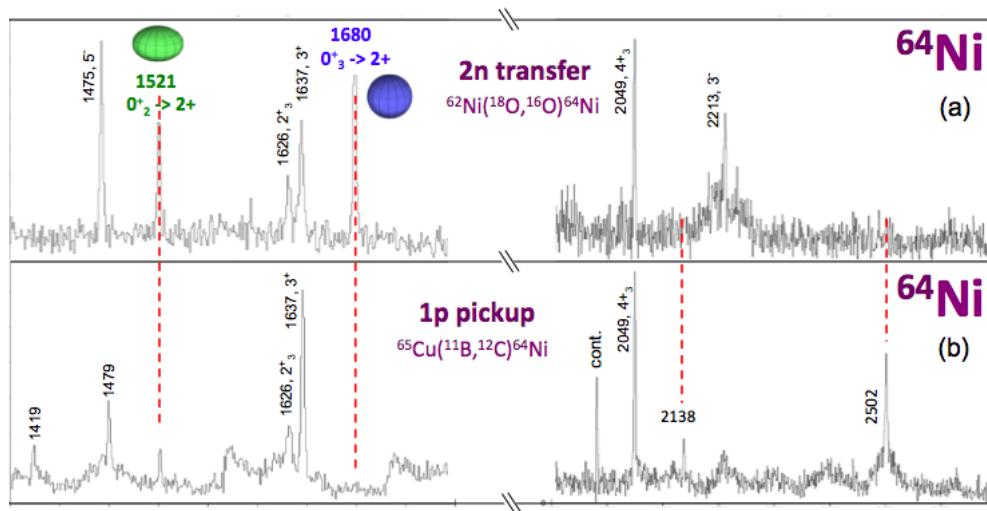


**Figure 5.** Portions of  $\gamma$  spectra of  $^{64}\text{Ni}$ , as obtained from the two-neutron transfer reaction  $^{62}\text{Ni}(^{18}\text{O},^{16}\text{O})^{64}\text{Ni}$  (a) and the proton-pick-up reaction  $^{65}\text{Cu}(^{11}\text{B},^{12}\text{C})^{64}\text{Ni}$  (b) (both performed at beam energies  $\sim 1$  MeV below the Coulomb barrier energy), focusing on the transition energy region where the decay from the second and third excited  $0^+$  states is expected. As in similar studies on  $^{62}\text{Ni}$  (see Fig. 4), a clear difference in population pattern is generally observed. In the case of the proton pick-up reaction, a strong suppression in the population of both negative parity states and  $0^+$  states is observed (see text for details).